CHAPTER 6

Hydrogen and methane rich syngas emission analysis through co-pyrolysis of low rank coal and de-oiled microalgae biomass*

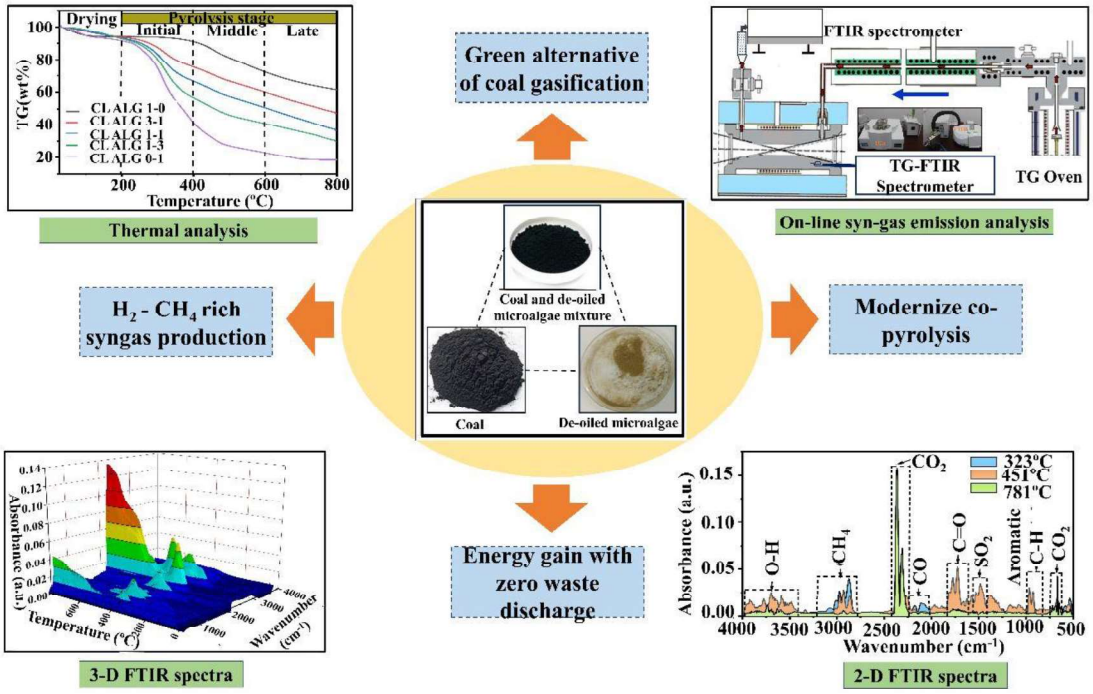

*This work is published in **Shweta Rawat and Sanjay Kumar (2024a)** Multi-objective genetic algorithm approach for enhanced cumulative hydrogen and methane rich syngas emission through co-pyrolysis of de-oiled microalgae and coal blending. Renewable Energy. 225, 120264.

Abstract

Towards establishing low-carbon bio-economy, the energy-rich syngas is considered a global energy carrier. Targeting hydrogen as a promising advanced fuel, the significance of methane also increases due to its direct conversion capability into hydrogen. The present chapter aims co-pyrolysis-based valorization of de-oiled microalgae and low-rank coal blend to generate H_2 and CH_4 rich syngas. Pyrolysis kinetic models, Kissinger-Akahira-Sunose (KAS) and Starink (STK) are used to evaluate apparent activation energy (E_a). The gradual addition of microalgae (0–100 %) in coal reduces E_a from 189.11–55.87 kJ/mol and 180.16–54.61 kJ/mol by KAS and STK method, respectively. The maximum hymethane carrying ratio is observed 2.51 and 3.51 at optimized conditions of response surface methodology (RSM) and artificial neural network-based multi-objective genetic algorithm (ANN-MOGA), respectively. Maximum H_2 (54.5 %) in the syngas is observed at mid pyrolysis stage (451 °C) using ANN-MOGA optimized conditions (blending ratio – 42.25 % and heating rate – 13.8 °C/min). This chapter highlights the advantage of ANN-MOGA optimization over statistical based optimization. Hence, incorporating the evolutionary algorithm as integrated ANN-MOGA optimization could be an efficient way to achieve hymethane-rich syngas emission in a co-pyrolysis approach to gain carbon-neutral energy with zero waste discharge.

6.1 Background

Towards global development of clean and sustainable energy system, biofuel production such as biohydrogen and biomethane has been considered the most demanding sustainable option (Li et al., 2024). Focusing on hydrogen as a promising advanced fuel, the importance of methane cannot be overlooked due to its direct conversion capability into hydrogen. As clean renewable energy carrier, biohydrogen and biomethane can be produced through thermochemical processes such as pyrolysis (Rawat and Kumar, 2023b). Fossil fuels (coal, fossil oil and natural gas), biomass (microalgae and lignocellulosic biomass) and industrial by-products (methanol and coke oven gas) are considered as potential pyrolysis feedstocks for hydrogen production (Tang et al., 2024). Among different conventional routes (water gas shift, steam reforming and partial oxidation), gasification is considered an established technology to produce syngas associated with major challenges such as maintenance of high pressure, high equivalence ratio, and high heat requirement (Zhou et al., 2024). To overcome these limitations of gasification, pyrolysis is recognized as a thermodynamically more stable technology with higher chemical potential efficiency to yield syngas at low environmental impact (Mavukwana et al., 2024). Recent studies of coal pyrolysis explored that low pyrolysis temperature (600-800°C) can improve the quantity and quality of syngas and other value-added end products (Yu et al., 2024). Compared to fossil fuel, biomass, specifically microalgae have been explored as a potential pyrolysis feedstock for syngas production with value added end products (Maliutina et al., 2018). The pressurized entrained-flow pyrolysis of *C. vulgaris* showed significant hydrogen production of 88 % (v/v) in bio-gas at 900 °C and 4 MPa (Maliutina et al., 2018). Further, pyrolysis of *Nannochloropsis sp.* in alkaline molten salt is explored to produce a high hydrogen yield of 71.48 mmol/g-algae

(Li et al., 2023). The catalytic pyrolysis of oleaginous microalgae, *Chromochloris zofingiensis* is reported hydrogen yield of 47.71 mmol/g-algae by using $Ni/Zr_{0.2}Ce_{0.8}O_2$ catalyst (Gao et al., 2024). Recently, surplus de-oiled microalgae biomass generation in biorefinery process is targeted for thermochemical conversion for further energy recovery aspect. The pyrolysis of de-oiled *C. sorokiniana* (Kumar et al., 2023), *Nannochloropsis* sp. (Lu et al., 2023), *C. pyrenoidosa* (Rawat and Kumar, 2023a) and *Scenedesmus* sp. (Mustapha et al., 2023) have been explored to produce bio-oil, syngas and biochar. Considering existing literature as a basis, research is strictly needed to emphasize syngas, specifically hydrogen and methane production and optimization through co-pyrolysis of fossil fuels and microalgae biomass for direct industrial-scale application (Mardani et al., 2019).

The machine learning approaches have drawn significant interest in thermal conversion processes such as pyrolysis for real-time monitoring, process optimization, product yield prediction and process control (Khan et al., 2024). After reviewing extensive pyrolysis studies, it was observed that syngas production and optimization through pyrolysis of different feedstocks using advanced machine learning tools are strictly lagging. Hence, the present chapter focuses on syngas emission analysis using co-pyrolysis of low-cost feedstocks (coal and de-oiled microalgae) and, further, maximizing energy-rich gases (biohydrogen and biomethane) using statistical as well as integrated ANN-MOGA model. As a global energy carrier, hydrogen-methane production and optimization are considered key objectives of the present chapter. In this direction, a novel approach is applied to maximize hydrogen and methane cumulatively in terms of the hymethane carrying ratio defined as $(H_2 + CH_4) / (CO + CO_2)$ by applying an optimization strategy. The present chapter covers real-time syngas emission analysis from pyrolysis feedstocks at different blending ratio and heating rate. Further, process parameters are optimized using statistical

and ANN-MOGA model to maximize hymethane carrying ratio. Then, syngas product distribution (H_2, CH_4, CO and CO_2) are analysed at different pyrolysis stages.

Present chapter explores co-pyrolysis of low rank coal and de-oiled microalgae as a sustainable approach to produce energy rich syngas in replacement of technically mature conventional coal gasification. Further, incorporation of intelligent modeling strategies of machine learning such as MOGA could aid advancements in pyrolysis technology to accelerate coal and de-oiled microalgae valorization to maximize H_2 and CH_4 rich syngas with the vision to establish zero waste discharge and bio-circular green economy.

6.2 Materials and methods

6.2.1 Feedstock processing and characterization of blended materials

The low rank coal as main pyrolysis feedstock material was obtained from Singrauli coalfield, India (latitude 2405′2.56″ N, longitude 82026′11.86″ E). Coal preprocessing, including screening, pulverization, and sieving (particle size < 0.25), was completed according to the standards of the American Society for Testing Materials (ASTM) as explained in previous section 5.2.1.

Freshwater microalgae, *C. pyrenoidosa* (NCIM 2738), was selected as co-material for pyrolysis with coal. The detailed protocol of microalgae cultivation, harvesting, de-oiling (Bligh and Dyer's method), and drying was also mentioned in earlier section 5.2.1. The de-oiled dried microalgae were sieved to achieve particle size < 0.60 mm. After preprocessing, de-oiled microalgae were blended with coal at the weight % of 0%, 25%, 50%, 75% and 100% expressed as blending ratio with notation of CL ALG 1-0, CL ALG 3-1, CL ALG 1-1, CL ALG 1-3, CL ALG 0-1, respectively in further experimental analysis. The blended coal and de-oiled microalgae powder was characterized through proximate, ultimate, and high heating value (HHV) analysis according to ASTM protocols such as ASTM D7582-15, ASTM D5373-14, and ASTM D5865-13, respectively.

6.2.2 Thermogravimetric and kinetic analysis

Thermogravimetric analyzer (TGA-50, Shimadzu, Kyoto, Japan) was used for TG experiments. The coal and/or de-oiled microalgae material (10.0 ± 0.2 mg) was used in hanging crucible made of aluminium with temperature increment from 30 to 800 °C at different heating rates of 10, 20, and 30 °C/min. The carrier gas (N_2) was purged at a 100 ml min^{-1} flow rate to maintain an inert pyrolysis environment (Rawat and Kumar, 2023a). In proceeding with TG analysis, kinetic analysis is also crucial for in-depth insights into applied chemical reactions and associated mechanisms during thermochemical degradation (Kumar et al., 2023b). Due to the high accuracy and independence of mechanism function or reaction order, isoconversional models have been successfully applied in different pyrolysis kinetic studies (Kumar et al., 2023b). The two isoconversional models, Kissinger-Akahira-Sunose (KAS) and Starink (STK), were utilized to calculate error-free E_a (Kumar et al., 2023b).

The conversion degree (α) and rate constant (k) during pyrolysis are expressed as Eq. 6.1 and 6.2, respectively.

$$\alpha = \frac{m_0 - m_t}{m_0 - m_f} \tag{6.1}$$

$$k = Aexp\left(\frac{-E_a}{RT}\right) \tag{6.2}$$

Where, m_o, m_t and m_f represents original mass, instantaneous mass at time t and final mass of sample, respectively. The A, E_a and T represents frequency factor, activation energy and pyrolysis temperature respectively.

The decomposition reaction rate can be represented as Eq. 6.3.

$$\frac{d\alpha}{dt} = kf(\alpha) \tag{6.3}$$

By substituting dT/dt (specified as heating rate, β), Eq. (3) can be turned into Eq. 6.4.

$$\beta\frac{d\alpha}{dt} = Aexp\left(-\frac{E_a}{RT}\right)f(\alpha) \tag{6.4}$$

The integral form of Eq. 6.4 is expressed as Eq. 6.5.

$$G(\alpha) = \int_0^{\alpha} \frac{d\alpha}{f(\alpha)} = \int_0^{T} \left(\frac{A}{\beta}\right) exp\left(-\frac{E_a}{RT}\right) dT = \left(\frac{AE_a}{\beta R}\right) P(u) \quad (6.5)$$

Where, $u = E_a/RT$, Eq. 6.5 can be solved by various *P (u)* equations resulting Doyle's equation (Eq. 6.6).

$$lnP(u) = 2.315 - 0.4567\frac{E_a}{RT} \quad (6.6)$$

In accordance with Eq. 6.6, mathematical expressions of KAS and STK are represented as Eq. 6.7 and Eq. 6.8, respectively (Kumar et al., 2023).

$$ln\left(\frac{\beta}{T^2}\right) = ln\left(\frac{AE_a}{RG(\alpha)}\right) - \frac{E_a}{RT} \quad (6.7)$$

$$ln\left(\frac{\beta}{T^{1.92}}\right) = C_s - 1.008\,\frac{E_a}{RT} \quad (6.8)$$

The linear plots of $ln\ (\beta/T^2)$ vs $1/T$ in Eq. (6.7) and $ln\ (\beta/T^{1.92})$ vs $1/T$ in Eq. (6.8) are used to calculate the E_a based on slope for the conversion degrees between 0.1 to 0.9.

6.2.3 TG-FTIR experiments

The thermogravimetric analyzer coupled with a Fourier-transform infrared spectrometer TG-FTIR (TGA 4000–Frontier FTIR, PerkinElmer, Waltham, Massachusetts, US) was used for simultaneous and real-time assessment of syngas emission during pyrolysis. The constant weight of 10 ± 0.2 mg was fed into the furnace of TG analyzer and temperature was increased from 30 to 800 ºC at uniform heating rate of 10 ºC/min to minimize heat transmission variation between different samples. As an agent gas, N_2 was passed through a furnace at a 100 ml min^{-1} flow rate to maintain anaerobic conditions. As the sample was heated, evolved gases were carried out of the furnace and directly transmitted to the FTIR spectrometer via a gas transfer line which was already heated at an internal temperature of 230 ºC. The FTIR spectrometer received spectra every 30 s and generated a continuous FTIR profile. The wavenumber range was set between 500 to 4000

cm^{-1} with a resolution of 4 cm^{-1} and 8 scans per sample. TG-FTIR analysis can continuously monitor the time-dependent evolution of gases and heavy liquid (Tar) evolution by analyzing functional groups in identifiable bands (Bassilakis et al., 2001).

6.2.4 Statistical analysis of coal and de-oiled microalgae blends thermal characteristic variables

One way analysis of variance (ANOVA) and Tukey's Honestly significant difference (HSD) test was performed to investigate statistical variation between different proximate-ultimate properties and E_a of coal and de-oiled microalgae blends by applying RStudio software (version 4.3.0). The statistical difference between the means of different groups was assessed by setting a significance level of $\alpha = 5\%$ with $p < 0.05$.

6.2.5 Response surface and statistical modeling

In statistics, RSM offers a practicable approach to optimizing stochastic functions (Sahoo et al., 2022). A multi-objective optimization study was performed by considering blending ratio and heating rate as significant process variables and hymethane carrying ratio at three pyrolysis characteristic temperatures (Tp_1, Tp_2, and Tp_3) as desired responses. The Design-Expert software version 13 (Stat-Ease, USA) was used for experiment designing using central composite design (CCD). It established 26 experimental runs, including 16 base runs and 10 centre points. The process variables with respective ranges are given in Table 6.1. Linear, quadratic, cubic and two factor interaction models for three responses are analyzed by using design expert software. Based on p value, quadratic model had been selected as suitable model for optimization. The ANOVA analysis was performed to distinguish well-fitted quadratic models based on Fischer test values (F-value) and probability values (p-value). The reliability and relevance of the model is decided based on higher F-value, and a lower p-value. Further, 3-D surface plots and contour plots are examined to analyze the individual and interactive effect of process variables upon desired responses.

Table 6.1 Experimental parameters and their levels to optimize hymethane carrying ratio via central composite design.

Independent variables	Units	Assigned code	Levels				
			-2	-1	0	1	2
Blending ratio	%	X_1	0	25	50	75	100
Heating rate	ºC/min	X_2	5	10	15	20	25

X_1 :Blending ratio (%); 0% : CL ALG 1-0; 25% : CL ALG 3-1; 50% : CL ALG 1-1; 75% : CL ALG 1-3; 100% : CL ALG 0-1; X_2 : Heating rate (ºC/min).

6.2.6 Artificial neural network aided multi-objective genetic algorithm model development

In thermal conversion processes such as pyrolysis, multi-task machine learning algorithms such as hybrid ANN-MOGA have revealed better performance for modeling mathematically complex, nonlinear and time-consuming processes with multiple advantages over conventional algorithms (Khan et al., 2024). MOGA integration with ANN facilitates better handling of present multi-variable and multi-optimization study with three desired outputs. Therefore, ANN-MOGA based machine learning tool is utilized to maximize hymethane carrying ratio at different characteristic temperature points.

To develop the ANN-MOGA model, total 52 experimental data sets were obtained from CCD matrix by conducting 26 runs of experiments in duplicate. These data input, had been further utilized for training, testing and validation of ANN model. The ANN model consists of two inputs (heating rate and blending ratio), three outputs (hymethane carrying ratio at Tp_1, Tp_2 and Tp_3 respectively) with one hidden layer consisting of ten neurons in between the input and output layer as shown in Fig. 6.1a–b. The MATLAB software version R2022b was used for model development. The Levenberg Marquardt (LM) algorithm with feed-forward backpropagation (FFBP) network technique was used in the ANN model. The FFBP network consists of multiple layers of interconnected neurons where information travels from input layer to output layer through the intermediate hidden layer (Yadav et al., 2023). In the ANN model, forward propogation calculates the error by adding all the inputs,

multiplying the random weights by bias and then applying it to the tangent sigmoid activation function (Saini et al., 2021). Model training using experimental datasets confirmed the weights that connect the layers. Further, error signal was calculated by utilizing the difference between the network's output and the desired output. The gradient descent method adjusted the weights in the direction of the negative gradient of the error function by minimizing the error between the network's output and the desired output. The backpropagation algorithm is an iterative process (Yadav et al., 2023). The weights were updated repeatedly until the mean square error (*MSE*) reached a minimum or a desired level of accuracy (Yadav et al., 2023).

Comparing predicted and experimental outcomes using a formula, a high-performance ANN model will show minimum *MSE* and high regression coefficient (R^2) as shown in Eq. 6.9 and Eq. 6.10, respectively.

$$MSE = \frac{1}{N}\sum_{i=1}^{n}(\alpha_i - \hat{\alpha}_i)^2 \quad (6.9)$$

$$R^2 = 1 - [\sum_{i=1}^{n}(\alpha_i - \hat{\alpha}_i)^2] / [\sum_{i=1}^{n}(\alpha_i - \bar{\alpha}_i)^2] \quad (6.10)$$

Where, α_i , $\hat{\alpha}_i$, and $\bar{\alpha}_i$ relate to experimental, predicted and average value of output.

The developed ANN model was further interlinked with a MOGA to optimize input factors to enhance hymethane carrying ratio. The MOGA populates the input variables effectively and consistently within a specified range from generation to generation and creates a function where the combination of multiple input variables denotes chromosome length (Saini et al., 2021). Each solution in the population was evaluated based on fitness function and solutions with higher fitness scores were selected to become parents of the next generation (Saini et al., 2021). These solutions undergo selection, crossover and mutation as a part of genetic algorithm's search process. Thus, genetic algorithm identified the promising solutions and gradually improved them over successive generations (Yadav

et al., 2023). In ANN, the weighted sum of inputs by a given node was passed through a non-linear activation function and output of one node acted as an input for another node in the next layer to compute the final ANN output.

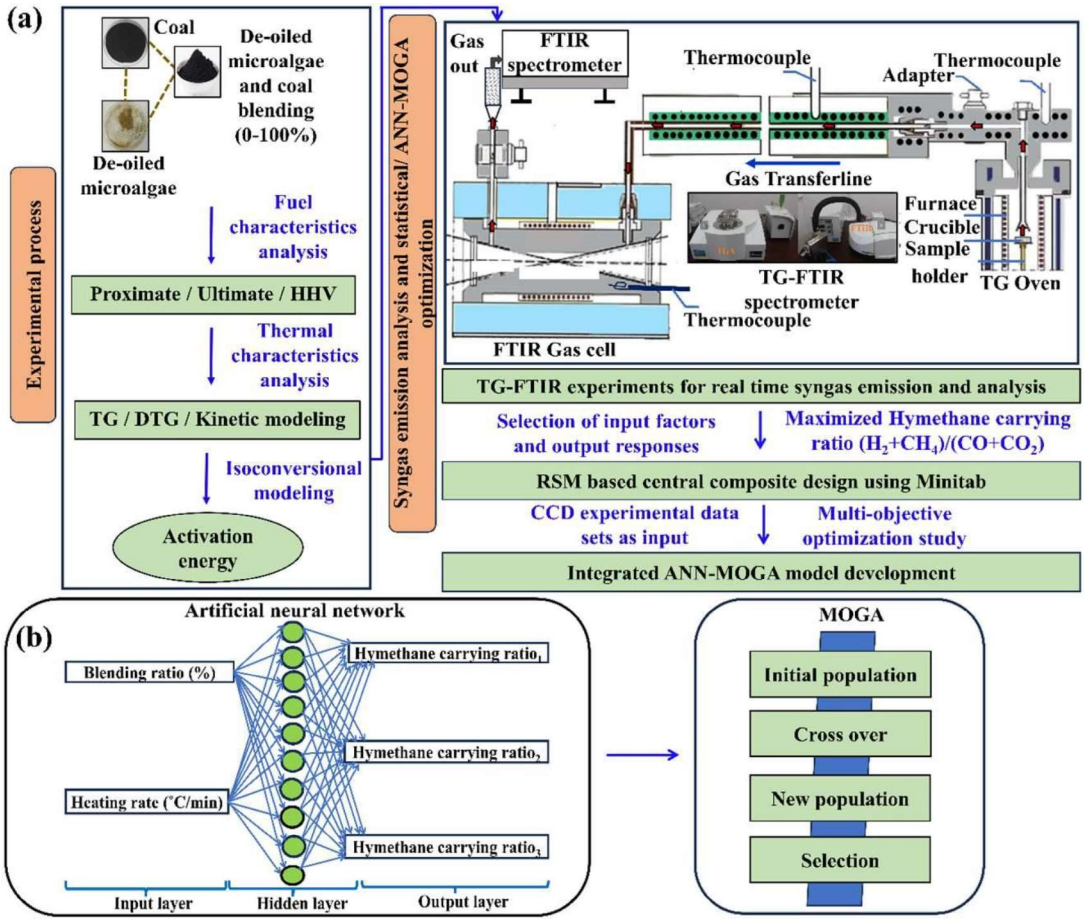

Fig. 6.1 Schematic representations (a) experimental work flow associated with optimization model development and validation (b) feedforward artificial neural network (ANN) architecture consisting of two neurons input layer, ten neurons hidden layer and three neurons output layer integrated with multi-objective genetic algorithm (MOGA) model.

The established ANN model was integrated with MOGA as an integrated ANN-MOGA to predict the optimal factor to enhance the hymethane carrying ratios at Tp_1, Tp_2 and Tp_3 as described in Eq. 6.11–6.13.

$$f_1 = max\ [ANNMOGA\ (1,1)] \tag{6.11}$$

$$f_2 = max\ [ANNMOGA\ (2,2)] \tag{6.12}$$

$f_3 = max\ [ANNMOGA\ (3,3)]$ (6.13)

Subject to: A∈ (0, 100); B∈ (5, 25)

The f signifies hymethane carrying ratio at pyrolysis characteristic temperature Tp_1, Tp_2 and Tp_3. The A and B denote input factors as blending ratio and heating rate, respectively. Model validation was accomplished by performing experiments in triplicates at ANN-MOGA optimized conditions. The detailed work flow and optimization strategy is represented in Fig. 6.1a –b.

6.3 Results and discussion

6.3.1 Fuel analysis

In fuel analysis, proximate results confirm that microalgae biomass having excess volatile matter (43%) and low ash content (18%) is suitable for co-pyrolysis with coal to produce high yield of syngas (Fig. 6.2a). Both feedstocks, coal and algae have moisture content less than 10 %. The moderate moisture content of both pyrolysis feedstocks favors H_2 and CO_2 production by targeting the possible conversion of H_2O to H_2 by water-gas shift reaction (Dominguez et al., 2008). Further, high volatile biomass content majorly contributes to gas emission and high fixed carbon content of coal associated with char as output (Nawaz et al., 2023). In elemental analysis, de-oiled microalgae showed a maximum mass loss of 82% with highest atomic H/C ratio of 1.76 (Fig. 6.2b). Higher H/C ratio of microalgae positively affects the syngas composition during pyrolysis and linearly correlated with H_2 emission. Further, negligible sulfur content of both pyrolysis feedstock, coal (< 1%) and microalgae (1.45%) indicate less SO_2 emission during co-pyrolysis. Tukey's HSD test (α = 5%) with $p < 0.05$ confirmed statistically significant variation for fuel properties between different pair of coal and de-oiled microalgae blends (Fig. 6.2a –b). The proximate and elemental analysis of coal and de-oiled microalgae blends is summarized in Table 6.2.

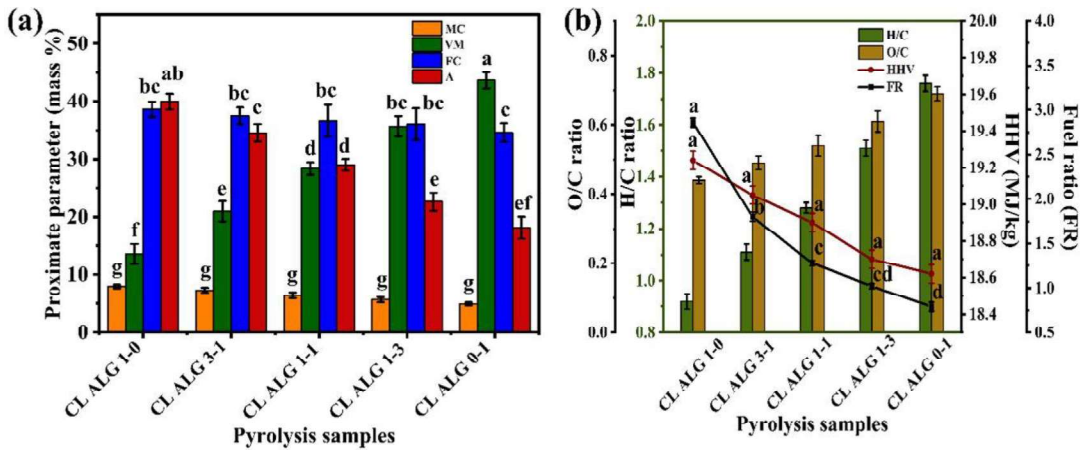

Fig. 6.2 Fuel analysis of coal and de-oiled microalgae blends (a) moisture content (MC), volatile matter (VM), fixed carbon (FC) and ash content (A) analysis (b) oxygen/carbon (O/C), hydrogen/carbon (H/C), fuel ratio (FR) and high heating value (HHV) analysis. Tukey's test (α = 5%) were performed with $p < 0.05$ among different groups.

Table 6.2 Fuel characteristic analysis of coal and de-oiled microalgae blends.

Samples	CL ALG 1-0	CL ALG 3-1	CL ALG 1-1	CL ALG 1-3	CL ALG 0-1
Proximate analysis (mass %)					
Volatile matter	13.50	20.80	28.30	35.40	43.01
Fixed carbon	38.60	37.48	36.20	36.19	34.05
Ash	40.0	34.51	29.0	22.50	18.0
Mineral matter[a]	44.0	37.96	31.90	25.85	19.80
Pyrite[b]	< 1.0	2.07	3.18	5.49	8.30
Fuel ratio[c]	2.86	1.80	1.28	1.02	0.79
High heating value (HHV- MJ/kg)	19.24	19.05	18.90	18.70	18.62
Elemental analysis (mass %)					
C	58.86	55.35	52.10	48.51	45.06
H	4.53	5.10	5.58	6.10	6.62
O	34.11	35.89	37.75	39.50	41.20
N	< 1.0	2.65	3.21	4.38	5.67
S	< 1.0	0.85	1.01	1.25	1.45
Atomic ratio					
H/C	0.92	1.11	1.28	1.76	1.76
O/C	0.44	0.49	0.54	0.69	0.69

All-observed values of responses were mean values of duplicates and standard deviation less than 3%; [a]Mineral matter mass % = 1.10. (Ash mass %); [b]Pyrite = 130. (S mass% – 0.30)/ Ash mass %; [c]Fuel ratio = Fixed carbon / Volatile matter.

6.3.2 Thermogravimetric analysis

The TG-DTG analysis for coal and de-oiled microalgae blended materials was performed in a thermogravimetric analyzer at 10 ºC/min with three main stages of pyrolysis as initial, middle, and late. The TG profile indicates high thermal activity of microalgal

biomass with lower ignition temperature (T_i) than coal (Fig. 6.3a). DTG profile represents that maximum degradation rate (DTG_{max}) for de-oiled microalgae was much higher (– 0.5 % /min) than coal (– 0.23 %/ min) which appeared at 311 ºC (Fig. 6.3b). The characteristic temperatures for thermal decomposition of coal and de-oiled microalgae blends are represented in Table 6.3.

Table 6.3 Estimation of characteristic temperatures for de-oiled microalgae and coal co-pyrolysis.

Samples (Heating rate-10°C/min)	Characteristic temperature points (ºC)				DTG_{max} (%/min)	W_R (%)
	T_i	T_{p1}	T_{p2}	T_{p3}		
CL ALG 1-0	335	464	ND	ND	0.21	61.58
CL ALG 3-1	268	319	452	735	0.26	47.39
CL ALG 1-1	253	315	448	748	0.31	37.00
CL ALG 1-3	247	313	445	747	0.42	29.49
CL ALG 0-1	240	311	442	754	0.50	18

T_i : initial temperature; T_{p1}, T_{p2} and T_{p3} : temperature of the first, second and third peak, respectively; DTG_{max} : mass loss rate of the first peak; W_R (%) : pyrolytic mass residue; ND : not detected.

In de-oiled microalgae, first sharp peak (311 ºC) was majorly related to the decomposition of residual lipid and saccharides, second peak (442 ºC) contributed to the protein decomposition and last weak peak (754 ºC) contributed to the inorganic material decomposition from char residues which is also confirmed by previous studies of microalgae pyrolysis (Kumar et al., 2023a). The DTG plots of coal-algae blends show two sharp and one weak peak corresponding to the individual pyrolysis contribution from coal and algae (Fig. 6.3b). In accordance with previous studies, DTG profile of coal shows single peak at temperature 464 ºC which indicates thermal resistance of coal as it is composed of aliphatic hydrocarbons, polycyclic aromatics, and oxygen-bearing heterocycle groups (Fig. 6.3b). As temperature increases, the oxidation of aliphatic hydrocarbons and aromatic ring structure causes a rapid decline in coal mass, similar to the

results of reported studies (Zhang et al., 2022). The thermal decomposition trend of blended feedstocks lies between coal and microalgae (Fig. 6.3a).

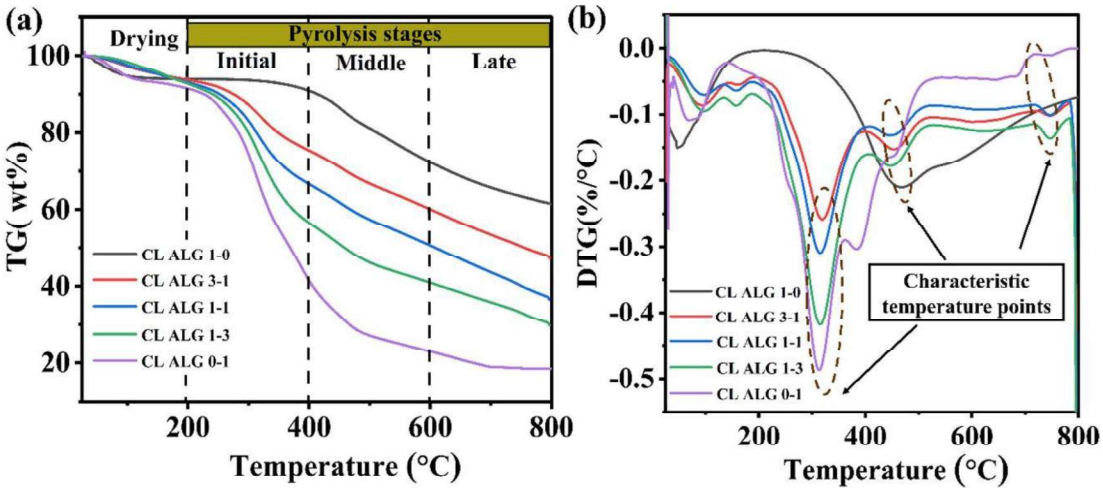

Fig. 6.3 (a) TG profile for coal and de-oiled microalgae blends (b) DTG profile for coal and de-oiled microalgae blends at heating rate (β) of 10 ºC/min.

6.3.3 Kinetic Analysis of coal and de-oiled microalgae blended material

Isoconversional approaches were used to evaluate E_a and R^2 through linear fitted plots of $ln(\beta/T^2)$ vs $10^3/T$ as in KAS method and $ln(\beta/T^{1.92})$ vs $10^3/T$ as in STK method for heating rates of 10, 20 and 30 ºC/min (Fig. 6.4). The conversion degree (α) between 0.1–0.9 was regarded for better data fitting and high R^2 value (Chen et al., 2020). At initial stage of microalgae pyrolysis (α = 0.1 to 0.4), E_a enhances due to decomposition of proteins and carbohydrates (Nawaz et al., 2023). Further, reduction in E_a was observed due to endothermic break down of specific constituents of microalgae at α = 0.4 to 0.7 (Nawaz et al., 2023). Finally, at α = 0.7 to 0.9, a sharp increment in E_a was observed due to enhanced char production with a steady decline in volatile matter (Nawaz et al., 2023). Similarly, the inconsistent fluctuation of E_a can be explained for coal and microalgae-coal blends at different extents of reaction. The progressive increase of microalgae addition in coal causes a gradual reduction in E_a of blends ranging from 189.11±24.84 kJ/mol (KAS) to 55.87±11.16 kJ/mol (KAS) and 180.16±25.80 kJ/mol (STK) to 54.61±11.97 kJ/mol (STK) (Table 6.4).

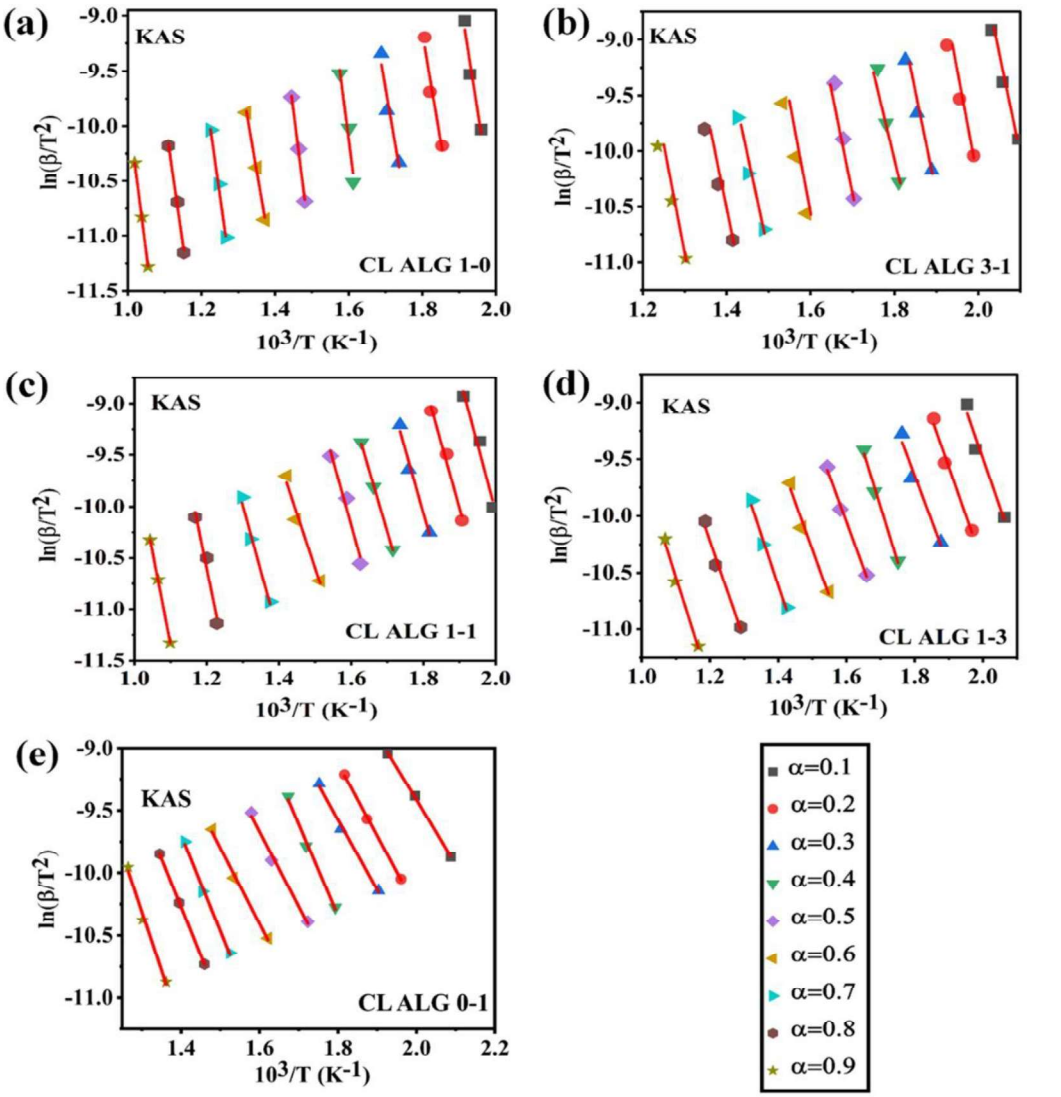

Fig. 6.4 Pyrolysis kinetic analysis over a range of mass conversion ratio (α = 0.1 to 0.9) by Kissinger - Akahira - Sunose (KAS) method.

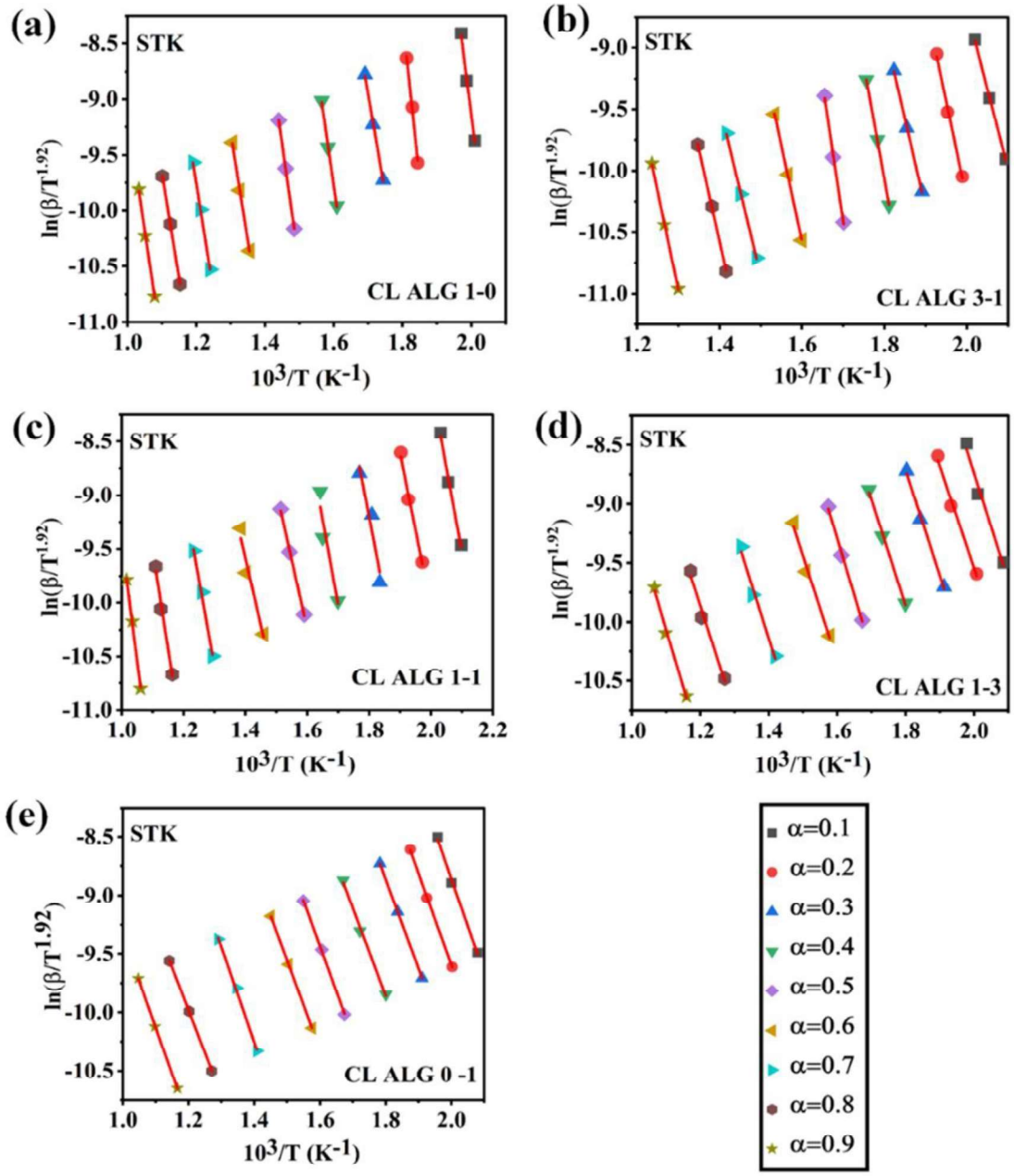

Fig. 6.5 Pyrolysis kinetic analysis over a range of mass conversion ratio (α = 0.1 to 0.9) by Starink (STK) method.

Table 6.4. Activation energy determination of de-oiled microalgae and coal blended material by using isoconversional KAS and STK method.

Sample	CL ALG 1-0				CL ALG 3-1			
	KAS		STK		KAS		STK	
α	E_a (kJ/mol)	R^2	E_a (kJ/mol)	R^2	E_a (kJ/mol)	R^2	E_a (kJ/mol)	R^2
0.1	161.04	0.92	158.77	0.99	128.87	0.99	110.14	0.99
0.2	161.62	0.92	163.64	0.98	143	0.98	123.82	0.98
0.3	176.17	0.92	176.09	0.99	149.4	0.98	132.05	0.98
0.4	214.67	0.92	178.40	0.99	151.31	0.99	152.05	0.99
0.5	216.25	0.99	199.19	0.99	160.46	0.99	182.92	0.99
0.6	161.04	0.99	173.18	0.99	152.06	0.99	123.06	0.99
0.7	193.63	0.99	164.96	0.99	149.74	0.99	143.17	0.99
0.8	197.62	0.98	165.95	0.99	150.02	0.99	148.31	0.99
0.9	219.99	0.99	241.25	0.99	165.45	0.99	183.85	0.99
Mean	189.11		180.16		150.03		144.37	
STD	24.84		25.80		10.31		25.79	
Sample	**CL ALG 1-1**				**CL ALG 1-3**			
0.1	98.11	0.93	98.63	0.99	65.68	0.92	60.42	0.96
0.2	103.59	0.96	101.45	0.98	73.16	0.97	73.73	0.98
0.3	104.54	0.96	117.95	0.99	76.90	0.97	74.38	0.99
0.4	108.30	0.99	118.37	0.99	80.15	0.99	75.33	0.99
0.5	142.50	0.93	120.19	0.99	68.83	0.99	77.41	0.99
0.6	98.94	0.97	98.37	0.99	67.75	0.98	65.82	0.97
0.7	103.59	0.94	100.63	0.99	72.33	0.98	73.82	0.97
0.8	150.23	0.99	145.46	0.99	74.83	0.98	74.49	0.97
0.9	150.64	0.99	145.63	0.99	83.97	0.97	79.07	0.97
Mean	117.83		116.29		73.73		72.72	0.98
STD	22.78		18.81		5.96		5.87	
Sample	**CL ALG 0-1**							
0.1	42.98	0.99	40.05	0.98				
0.2	46.46	0.99	43.18	0.99				
0.3	48.05	0.99	45.75	0.99				
0.4	63.93	0.99	63.92	0.99				
0.5	60.63	0.99	58.29	0.99				
0.6	50.28	0.99	50.47	0.99				
0.7	49.46	0.99	49.32	0.99				
0.8	63.68	0.98	63.51	0.99				
0.9	77.32	0.98	77.0	0.99				
Mean	55.87		54.61					
STD	11.16		11.97					

α : Degree of conversion; KAS : Kissinger-Akahira-Sunose method; STK : Starink method; E_a : activation energy; R^2 : correlation coefficient.

These results indicate a significant impact of microalgae addition to blends in form of gradual E_a reduction and higher thermochemical performance (Fig. 6.6a). Both kinetic models show nearly identical fluctuation patterns (Fig. 6.6b).

Further, the co-pyrolysis process is considered a multistep complex reaction attributed by parallel, competitive and consecutive reactions resulting from a fluctuated E_a pattern (Nawaz et al., 2023). The Tukey's HSD test (α = 5%) confirms that within the group, E_a evaluated by KAS and STK method is statistically similar. However, significant differences in mean values for E_a are observed between different groups. The E_a found in the present research are consistent with earlier reported co-pyrolysis studies of *Spirulina* with low rank coal (Wu et al., 2017), *Nannochloropsis* sp. with Colombian bituminous coal (Fermoso et al., 2018) and *Scenedesmus* sp. with bituminous coal (Nyoni et al., 2023).

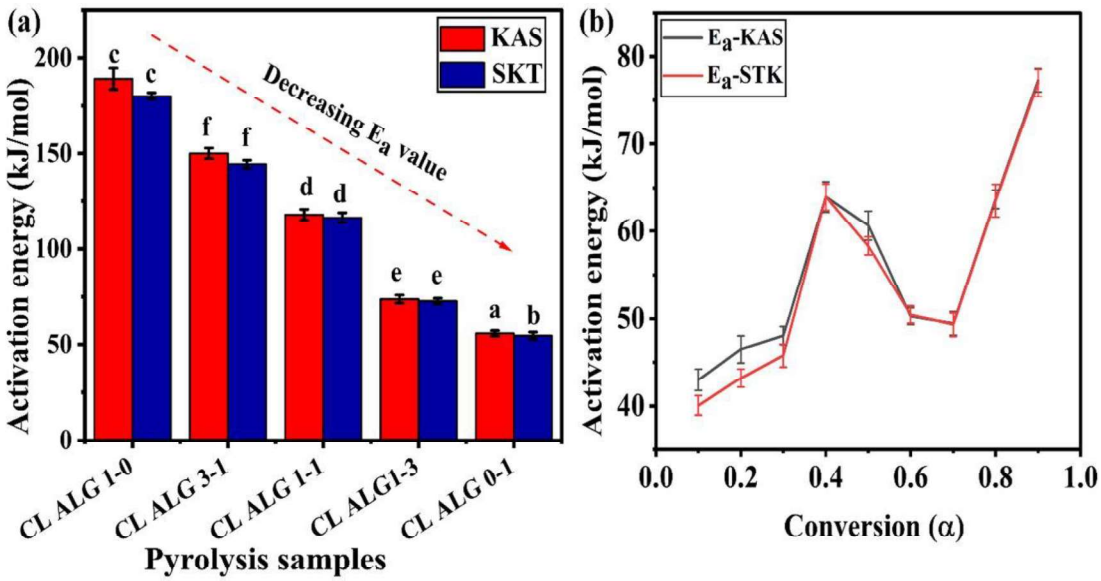

Fig. 6.6 Activation energy (E_a) estimation for (a) coal and de-oiled microalgae blends (b) individual de-oiled microalgae over a range of mass conversion ratio (α=0.1 to 0.9) by using Kissinger-Akahira-Sunose (KAS) method and Starink (STK) method. Tukey's test (α = 5%) was performed with $p < 0.05$ among different groups.

6.3.4 Syngas emission analysis during co-pyrolysis of coal and de-oiled microalgae blended material

Due to multistage coupling and crosslinking reactions, it is not possible to deconvolute primary reactions from secondary reactions during volatile gas emission (Song et al., 2017). Therefore, coupled TG-FTIR-based hyphenated method was applied to provide dynamic distribution of functional groups of emitted gases with respect to time and temperature variation (Ong et al., 2020). The main FTIR absorption peaks were detected at 3800–3500 cm^{-1}, 3180–2600 cm^{-1}, 2410–2240 cm^{-1}, 2240–2030 cm^{-1}, and 780–600 cm^{-1} for different blends (Fig. 6.7 a–e). The peaks at 3800–3500 cm^{-1} attribute to dehydration reaction with possible end products of H_2 (Wu et al., 2022). During microalgae pyrolysis (at Tp_1 and Tp_2), carbohydrate and lipid breakdown contribute to two distinct absorption peaks between 3180 cm^{-1} and 2600 cm^{-1} due to C-H stretching vibration with possible end product as CH_4 (Kumar et al., 2023b).

The significant characteristic peaks at 2410–2240 cm^{-1} and at 755 cm^{-1}/565 cm^{-1} are attributed to COOH and C=O groups, respectively, confirming CO_2 emission (Liu et al., 2020). A significant peak at 1762 cm^{-1} validates the decomposition of protein and carbohydrate (Kumar et al., 2023b). Further, NH_3 emission due to possible deamination reaction is confirmed by presence of a prominent peak at 966 cm^{-1} (Kumar et al., 2023b). The characteristic peak at 1472 cm^{-1} confirms the presence of organic sulfate responsible for the end product SO_2 (Song et al., 2017). The thermal stability order of function groups was reported as – OH > – COOH > – O–CH_3, which causes significant emission of H_2 at higher temperatures (middle and late pyrolysis stage) than CH_4, which is completely emitted till middle pyrolysis (Wu et al., 2018). During coal pyrolysis, thermal cracking of the aliphatic side chain is mainly responsible for rich CH_4 emission (nearly 50.49% of overall gaseous product), which is missing in microalgae pyrolysis.

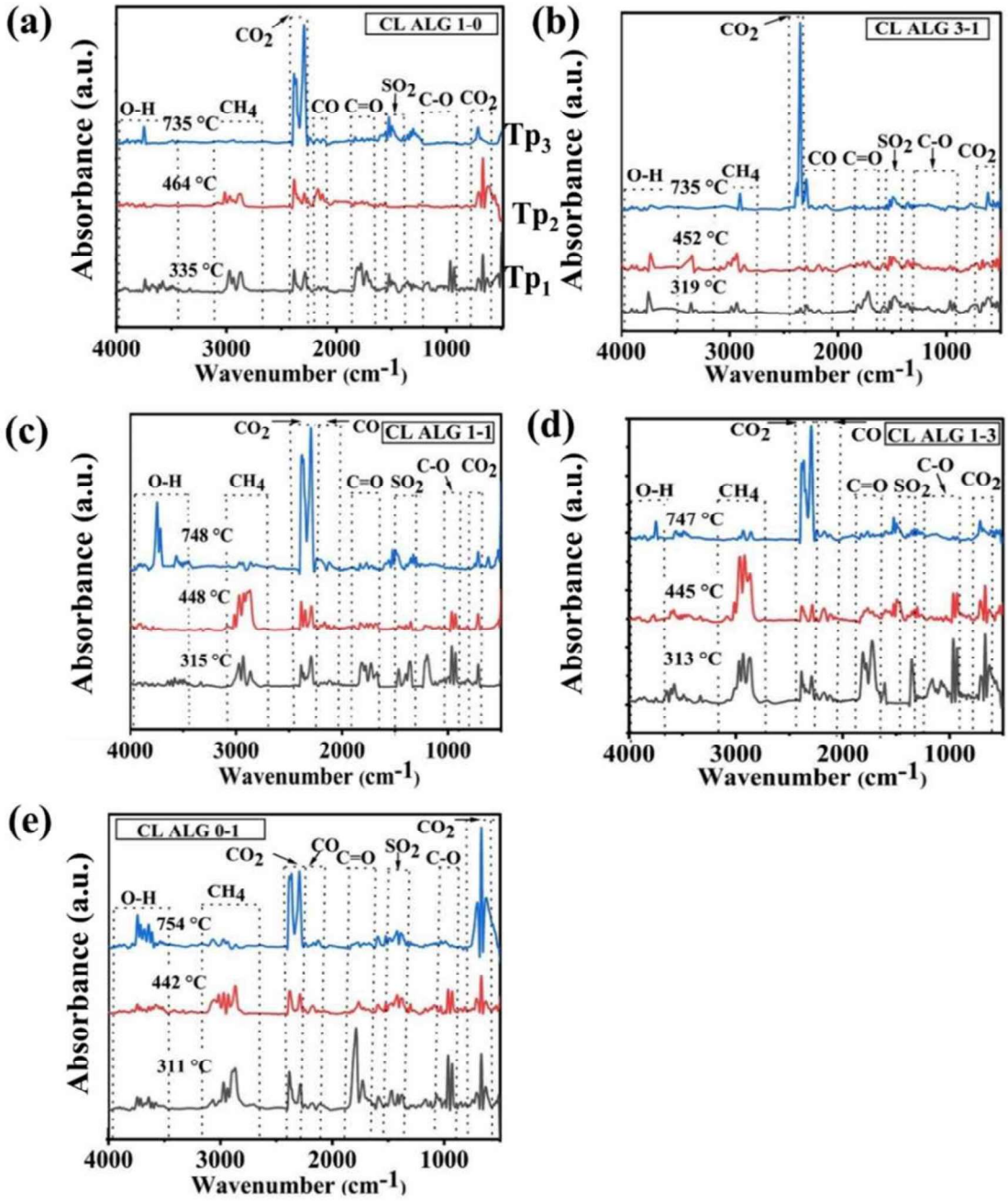

Fig. 6.7 Syngas emission analysis by TG-FTIR at pyrolysis characteristic temperatures for coal and de-oiled microalgae blends (a) CL ALG 1-0 (b) CL ALG 3-1 (c) CL ALG 1-1 (d) CL ALG 1-3 (e) CL ALG 0-1.

6.3.5 Statistical optimization of process variables to enhance hymethane carrying ratio and analysis

The co-pyrolysis experiments were conducted based on the CCD design matrix, and responses were recorded as hymethane carrying ratio at three characteristic temperatures (Table 6.5). To determine the effect of process variables defined as blending ratio and heating rate upon measured responses, multiple regression analysis was performed by using experimental data (Table 6.6). Regression analysis indicated the statistical significance ($p < 0.001$) of all probable relationships, linear, quadratic, and interactive terms of blending ratio and heating rate for hymethane carrying ratio estimation (Table 6.6). Quadratic polynomial equations were established via regression coefficients calculation to determine hymethane carrying ratio at characteristic temperatures (Table 6.7). Further, reliability of the model was evaluated based on p and F value tests of ANOVA results (Table 6.8).

The designed model is statistically reliable with maximum F value of 189.54 and minimum p-value of < 0.001 for hymethane carrying ratio estimation. There was only 0.01% chance that this model F- value could occur due to noise. The R^2 value for hymethane carrying ratio at different characteristic temperatures was 0.95–0.98 (close to one), confirming the excellent model approximation. The interactive effect of process variables, blending ratio and heating rate on the hymethane carrying ratio are represented by three-dimensional surface plots (Fig. 6.8). Further, it is observed that increasing microalgae blending ratio (0–100%) shows a sharp uptrend in hymethane carrying ratio as 0.29 to 1.11, 0.58 to 3.02 and 0.024 to 0.5 at Tp_1, Tp_2 and Tp_3 (Fig. 6.8 a–c).

Table 6.5 A two-level full-factorial central composite design matrix in real value and coded unit (in parenthesis) with different responses for syngas production during co-pyrolysis of de-oiled microalgae, coal, and blends.

Runs	Process parameters		Response variable		
	Blending ratio (%)	Heating rate (°C/min)	Hymethane carrying ratio $[(H_2+CH_4)/(CO+CO_2)]$		
	X_1	X_2	Y_1	Y_2	Y_3
1.	25 (–1)	10 (–1)	0.74±0.05	1.49±0.05	0.44±0.03
2.	25 (–1)	10 (–1)	0.82±0.08	1.43±0.08	0.5±0.07
3.	75 (+1)	10 (–1)	0.66±0.07	1.84±0.08	0.11±0.01
4.	75 (+1)	10 (–1)	0.58±0.08	1.76±0.07	0.07±0.005
5.	25 (–1)	20 (+1)	0.68±0.04	2.9±0.01	0.11±0.04
6.	25 –1)	20 (+1)	0.61±0.06	2.89±0.01	0.05±0.003
7.	75 (+1)	20 (+1)	1.10±0.08	1.36±0.07	0.43±0.07
8.	75 (+1)	20 (+1)	1.02±0.09	1.28±0.03	0.37±0.06
9.	0 (–α)	15 (0)	0.64±0.07	1.62±0.07	0.45±0.05
10.	0 (–α)	15 (0)	0.70±0.01	1.70±0.08	0.37±0.02
11.	100 (+α)	15 (0)	0.97±0.05	1.07±0.07	0.44±0.07
12.	100 (+α)	15 (0)	0.89±0.07	1.0±0.08	0.39±0.05
13.	50 (0)	5 (–α)	0.37±0.04	0.65±0.01	0.04±0.001
14.	50 (0)	5 (–α)	0.29±0.01	0.58±0.03	0.02±0.002
15.	50 (0)	25 (+α)	0.65±0.07	0.84±0.08	0.14±0.02
16.	50 (0)	25 (+α)	0.71±0.08	0.81±0.03	0.12±0.01
17.	50 (0)	15 (0)	1.02±0.05	3.02±0.15	0.29±0.03
18.	50 (0)	15 (0)	1.01±0.08	3.0±0.20	0.30±0.01
19.	50 (0)	15 (0)	0.97±0.07	2.99±0.10	0.28±0.02
20.	50 (0)	15 (0)	0.98±0.04	3.01±0.50	0.29±0.03
21.	50 (0)	15 (0)	1.04±0.08	2.98±0.10	0.31±0.04
22.	50 (0)	15 (0)	0.98±0.04	3.02±0.25	0.27±0.01
23.	50 (0)	15 (0)	1.03±0.09	3.01±0.40	0.32±0.03
24.	50 (0)	15 (0)	1.11±0.15	2.98±0.15	0.28±0.02
25.	50 (0)	15 (0)	1.04±0.08	2.97±0.25	0.28±0.04
26.	50 (0)	15 (0)	1.05±0.07	3.01±0.15	0.32±0.05

X_1 : Blending ratio (%); X_2 : Heating rate (◦C/min); Y_1, Y_2 and Y_3 : hymethane carrying ratio at Tp_1, Tp_2 and Tp_3 respectively (mean values of duplicates ±standard deviation); Blending ratio 0% : CL ALG 1–0; 25% : CL ALG 3–1; 50% : CL ALG 1-1; 75% : CL ALG 1–3; 100% – CL ALG 0–1.

Table 6.6 Model coefficient estimation by multiple regression analysis for enhancing hymethane carrying ratio at different pyrolysis characteristic temperatures.

Model	Y_1				Y_2				Y_3			
	Coef	SE	t	P	Coef	SE	t	P	Coef	SE	t	p
Constant	1.07	0.016	62.97	< 0.001	2.96	0.04	44.30	< 0.001	0.29	0.011	27.39	<0.001
X_1	0.06	0.011	5.81	< 0.001	–0.21	0.03	–5.37	< 0.001	–0.00	0.0073	–0.54	< 0.001
X_2	0.08	0.011	7.54	< 0.001	0.12	0.03	3.41	< 0.001	0.009	0.007	1.25	< 0.001
X_1^2	–0.06	0.008	–7.07	< 0.001	–0.42	–0.02	–12.23	< 0.001	0.029	0.005	5.51	< 0.001
X_2^2	–0.13	0.008	–16.2	< 0.001	–0.57	–0.02	–16.80	< 0.001	–0.05	0.005	–9.95	< 0.001
$X_1 X_2$	0.14	0.019	7.47	< 0.001	–0.48	–0.05	–7.56	< 0.001	0.17	0.013	13.63	< 0.001

X_1 : blending ratio (%); X_2 : heating rate (º C/min); Coef : coefficient; SE : standard error; Blending ratio 0% : CL ALG 1–0; 25% : CL ALG 3–1; 50% : CL ALG 1–1; 75% : CL ALG 1–3; 100% – CL ALG 0–1.

Table 6.7 Quadratic polynomial equations for enhancing hymethane carrying ratio at different pyrolysis characteristic temperatures.

Coded term:	
$Y_1 =$	$1.006 + 0.064\,X_1 + 0.083\,X_2 - 0.057\,X_1^2 - 0.13\,X_2^2 + 0.14 X_1 X_2$
$Y_2 =$	$2.96 - 0.208\,X_1 + 0.115\,X_2 - 0.415\,X_1^2 - 0.572\,X_2^2 - 0.48 X_1 X_2$
$Y_3 =$	$0.2912 - 0.004\,X_1 + 0.0092\,X_2 + 0.029\,X_1^2 - 0.053\,X_2^2 + 0.175\,X_1 X_2$

X_1 : blending ratio (%); X_2 : heating rate (º C/min); Coef : coefficient; SE : standard error; Blending ratio 0% : CL ALG 1–0; 25% : CL ALG 3–1; 50% : CL ALG 1-1; 75% : CL ALG 1–3; 100% – CL ALG 0–1.

The optimization results indicated that at initial and last pyrolysis stage, microalgae blending ratio is main contributor to enhance hymethane carrying ratio. However, in the middle stage, pyrolysis temperature and heating rate are more influential than blending ratio. During co-pyrolysis, microalgal biomass reacts with an inert gas stream and cause tar production as by-products along with syngas (Gan et al., 2021). Dehydrogenation reactions related to protein degradation and phenyl group depolymerization mainly contribute to H_2 emission (Wu et al., 2015). As a secondary reaction, tar cracking at higher temperatures promotes H_2 production (Gan et al., 2021).

Table 6.8 Analysis of variance for enhancing hymethane carrying ratio at different pyrolysis characteristic temperatures.

Source	df	Y_1				Y_2				Y_3			
		SS	MS	F	P	SS	MS	F	P	SS	MS	F	p
Model	5	1.23	0.25	83.39	< 0.001	21.39	4.28	189.54	< 0.001	0.47	0.095	72.45	< 0.001
X_1	1	0.10	0.10	33.81	< 0.001	1.03	1.03	45.78	< 0.001	0.0004	0.0004	0.29	< 0.001
X_2	1	0.17	0.17	56.86	< 0.001	0.32	0.32	14.06	< 0.001	0.002	0.002	1.57	< 0.001
X_1X_2	1	0.17	0.17	55.84	< 0.001	1.84	1.84	81.66	< 0.001	0.24	0.24	185.81	< 0.001
X_1^2	1	0.15	0.15	49.96	< 0.001	7.91	7.91	350.35	< 0.001	0.04	0.04	30.32	< 0.001
X_2^2	1	0.78	0.78	263.86	< 0.001	15.01	15.01	664.93	< 0.001	0.13	0.13	99.06	< 0.001
Error	20	0.059	0.0029			0.45	0.023			0.026	0.0013		< 0.001
Lack-	3	0.022	0.007	3.24	0.048	0.43	0.14	124.58	< 0.001	0.013	0.0042	5.16	< 0.001
Pure	17	0.038	0.002			0.02	0.001			0.014	0.0008		
Total	25	1.29				21.84				25	0.50		
R^2	0.95					0.98				0.95			

X_1 : blending ratio (%); X_2 : heating rate (º C/min); *df* : degree of freedom; *SS* : sum of square; Y_1, Y_2 and Y_3 : hymethane carrying ratio at Tp_1, Tp_2 and Tp_3, respectively; Blending ratio 0% : CL ALG 1–0; 25% : CL ALG 3–1; 50% : CL ALG 1-1; 75% : CL ALG 1–3; 100% – CL ALG 0–1.

In syngas emission, methane plays a significant role in enhancing hymethane carrying ratio. In agreement of previous studies, the cracking of mono/ polysaccharides and residual lipids is majorly responsible for CH_4 emission during microalgae pyrolysis (Gan et al., 2021). Further, CO_2 is also the major component of syngas emission, derived from proteins and carbohydrates decomposition. As suggested by other studies, CO production and emission are less significant than CO_2 emission in coal and de-oiled microalgae pyrolysis (Wu et al., 2015). A non-linear impact of heating rate can be seen upon co-pyrolysis of coal and de-oiled microalgae Fig. 6.8 a–c. Considering the heterogeneous structure of coal and microalgae biomass, a very inconsistent impact of heating rate can be observed. At a very low heating rate (5–10 ºC/min), mass and heat transfer are very limiting across the pyrolysis feedstock (Hong et al., 2017). However, increasing heating rate (10–20 ºC/min) overcame mass and heat transfer limitations, leading to higher thermal conversion during pyrolysis (Wu et al., 2018b). Besides pyrolysis temperature, the heating rate

significantly influences bio-oil and syngas emissions yield. Within a certain range, higher heating rates positively affect the yield of syngas and negatively impact liquid products.

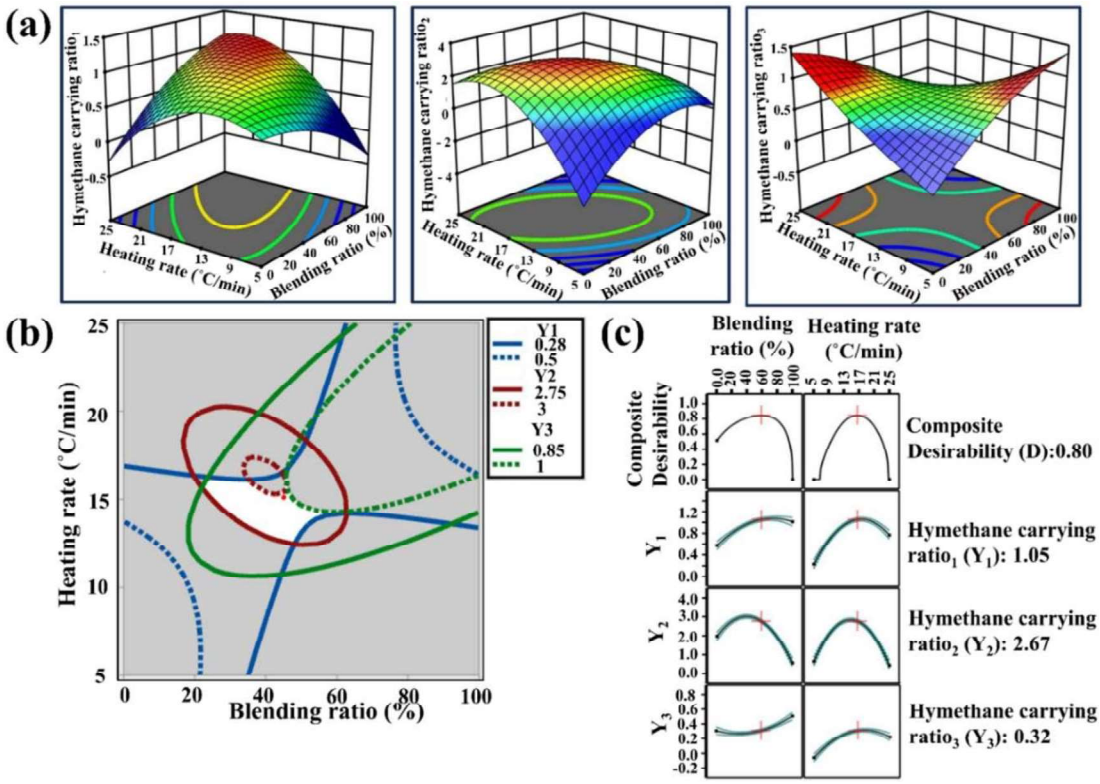

Fig. 6.8 RSM-based CCD optimization (a) 3-D response surface plots (b) overlaid contour plot (c) multi-objective optimization plot to maximize Y_1, Y_2 and Y_3 – hymethane carrying ratio at Tp_1, Tp_2 and Tp_3 respectively. Blending ratio 0% : CL ALG 1–0; 25% : CL ALG 3–1; 50% : CL ALG 1-1; 75% : CL ALG 1–3; 100% – CL ALG 0–1.

The combined contribution of blending ratio and heating rate were analyzed to maximize the hymethane carrying ratio at Tp_1, Tp_2 and Tp_3 by using the composite desirability function approach. The optimum composite desirability value was 0.80, which fulfills 80.0 % of the maximum obtainable response for each variable. All three responses related to hymethane carrying ratio were overlaid using the regression analysis equation (Table 6.7). Further, the overlaid contour plot was established to visualize a common feasible region to maximize the responses as shown in Fig. 6.8b. The RSM based optimization predicts blending ratio–58.66% and heating rate–16.5 ºC/min for

maximization of hymethane carrying ratios. As a limitation, 3D or 2D diagram may be represented by considering two experimental factors simultaneously.

6.3.6 Integrated ANN-MOGA model development for hymethane enhancement

To establish ANN-MOGA model, CCD experimental data sets, including input variables and output responses, were employed for training, testing and validation of ANN model. Multi-objective optimization facilitates non-dominated multiple optimization data sets as an optimal solution for handling multiple objectives (Saini et al., 2021). Further, selection of single data set is based on feasibility and requirement of current problem (Chhabra et al., 2014). In ANN model, FFBP network consists of multiple layers of interconnected neurons where information travels from input layer to output layer through hidden layers (Yadav et al., 2023). In current study, the model consists of an input layer (three neurons), one hidden layer (ten neurons) and output layer (three neurons). The random division of total 26 experiments was utilized as: 18 for training the model, 4 for testing the model's performance and 4 for model validation. In ANN, the tangent sigmoid activation function was utilized to obtain regression plots with high R^2 values of 0.9989, 0.9989, 0.9955 for training, testing, and validation stages, respectively (Fig. 6.9e). The gradient and validation checks show that iterations stop at 6 after attaining the minimum *MSE* at epoch 4 (Fig. 6.9d). The performance graph shows that best validation performance has been achieved at epoch 4 with a minimum *MSE* of 0.00132 (Fig. 6.9c). Along with a high regression coefficient and minimum *MSE* value, error histogram plots depict the error of 0.007 between the ANN predicted and experimentally obtained target values (Fig. 6.9a). Therefore, the overall R^2 obtained from the proposed model is 0.9983, which indicates the robustness of the developed model.

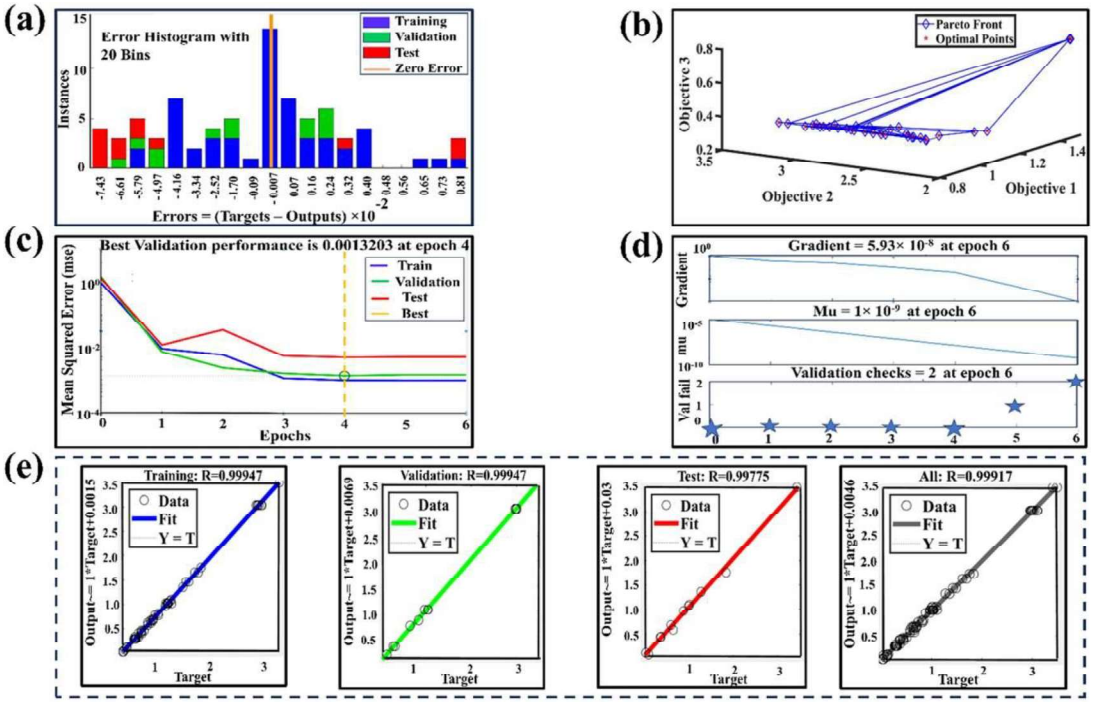

Fig. 6.9 ANN-MOGA modeling to enhance hymethane carrying ratio (a) error histogram (b) pareto front for multi-objective optimization (c) mean square error vs epoch plot (d) performance through validation check plot (e) regression plots displaying training, validation and test models with regression coefficient values.

Further, a MOGA function was integrated with ANN to result a hybrid ANN-MOGA model and passed through a number of runs in MATLAB to obtain optimum input values to maximize desired multi-responses. The population size is set as 100, which is mostly random. The chromosome length is represented by the row of population, which shows input factors within the given range. Every chromosome length is incorporated into the fitness function. Further, a trained ANN model obtained from LM and FFBP algorithm (Chhabra et al., 2014). It randomly populates offspring with two-point crossover and mutation operation. Mutation rate, crossover fraction, and elite count were essential GA factors set as 0.01, 0.8, and 2, respectively. In the present MOGA optimization, three pareto front in space stands for a set of non-linear solutions for three objective functions that are non-dominant to each other but are superior to the rest of the solutions in the search space as shown in Fig. 6.9b. This model provides seventy non-dominant optimization data sets as

optimal solutions, out of which one selected data set is considered as most suitable for further validation of the optimization model. The present ANN-MOGA model predicts optimized input variables as a blending ratio of 42.25 % and heating rate of 13.79 ºC/min for maximum hymethane carrying ratio at Tp_1, Tp_2, and Tp_3, respectively (Table 6.9).

Table 6.9 Comparison of hymethane carrying ratio from co-pyrolysis of coal-microalgae blends at different optimization conditions.

	Process condition		**Pyrolysis characteristic peak temperatures**			**Hymethane carrying ratio**		
	Blending ratio (%)	**Heating rate (ºC/min)**	**Tp_1**	**Tp_2**	**Tp_3**	***Y_1***	***Y_2***	***Y_3***
CL ALG 1-1 (Blending ratio 50%)	50.0	15.0	315	448	748	1.02	1.88	0.25
Statistical optimized	58.66	16.5	329	455	775	1.92	2.51	0.31
ANN-MOGA optimized	42.25	13.8	323	451	781	2.01	3.51	0.35

Blending ratio 0% : CL ALG 1–0; 25% : CL ALG 3–1; 50% : CL ALG 1-1; 75% : CL ALG 1–3; 100% : CL ALG 0–1; Y_1, Y_2, Y_3 : Hymethane carrying ratio at Tp_1, Tp_2 and Tp_3 respectively.

6.3.7 Model validation and comparative assessment of RSM and ANN-MOGA

RSM and ANN-MOGA model are utilized to determine optimal data points of input variables to maximize hymethane carrying ratio at different characteristic temperatures. The validation experiments were conducted in triplicate at RSM based CCD optimized process conditions: blending ratio – 58.66 % and heating rate – 16.5 ºC/min. The experimental results showed a hymethane carrying ratio of 1.92, 2.51, and 0.31 at Tp_1, Tp_2, and Tp_3, respectively, which is slightly different and consistent with predicted RSM results (Table 6.9). Further, similar experiments were repeated at ANN-MOGA evaluated process conditions; blending ratio – 42.25 % and heating rate – 13.8 ºC/min, which showed hymethane carrying ratio of 2.01, 3.51, and 0.35 at Tp_1, Tp_2, and Tp_3 respectively (Table 6.9 and Fig. 6.10). Further, experimental results for CL ALG 1-1 sample (blending ratio – 50%, heating rate – 15 ºC/min) provide very inferior results as hymethane carrying ratio of

1.02, 1.88 and 0.25 at Tp_1, Tp_2, and Tp_3 respectively (Table 6.9 and Fig. 6.10). The statistically significant variation for hymethane carrying ratio at different process conditions is confirmed by Tukey's HSD test ($\alpha = 5\%$) with $p < 0.05$ (Fig. 6.10).

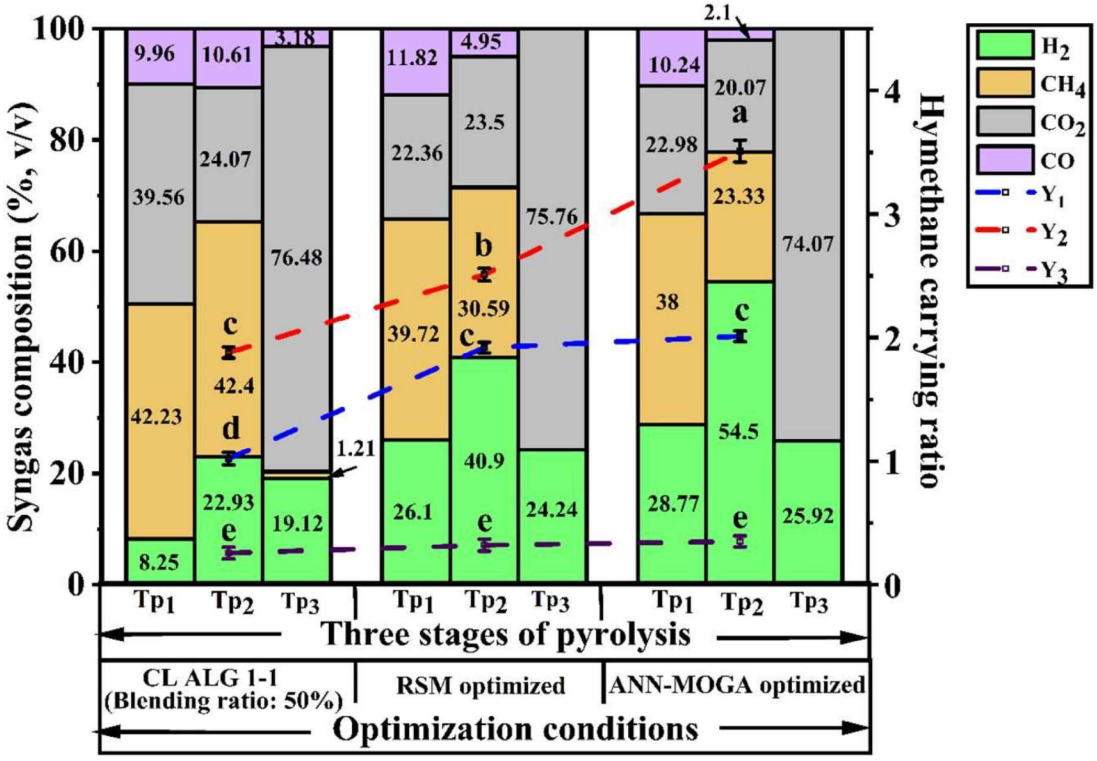

Fig. 6.10 Experimental validation of hymethane carrying ratio and syngas distribution at (a) CL ALG 1-1 (blending ratio: 50%) (b) statistical optimized (RSM) (c) ANN - MOGA optimized condition. Tukey's test ($\alpha = 5\%$) was performed with $p < 0.05$ among different groups.

These results revealed that ANN-MOGA generated optimization conditions provide higher hymethane carrying ratio at three different characteristic temperatures than RSM-based process conditions. The reason is that RSM assumes a quadratic relationship between variables and response, which limits its performance when dealing with intricate interactions in the pyrolysis process (Zhan et al., 2024). In contrast, ANN can model complex, non-linear or dynamic relationships with high prediction accuracy (Zhan et al., 2024). To handle present multi-objective optimization problem with high dimensionality and potential discontinuities in response surface, ANN-MOGA efficiently explores the

parameter space and mitigate the limitations of single-point search algorithms (Saini et al., 2021).

In-depth comparative assessment of RSM and ANN-MOGA performance is determined based on syngas product distribution (H_2, CH_4, CO_2, and CO) at three stages of pyrolysis for different optimization conditions. The maximum H_2 – 54.5% was achieved at 451 ºC temperature, performing co-pyrolysis at ANN-MOGA optimized process conditions (Fig. 6.10). This H_2 emission is 13.6 % higher than H_2 % at RSM optimized process conditions. Recently, pyrolysis of de-oiled *C. sorokiniana* was reported, claiming 44.46 % H_2 emission under optimized conditions (Kumar et al., 2023b). Further, H_2 emission in other pyrolysis and gasification studies is analyzed. In this direction, a gasification study is reported to emit 42.88 % H_2 by loading 3 g of sugarcane bagasse at 900 ºC and 30 min reaction time (Raheem et al., 2019). The gasification of *C. vulgaris* is reported to emit optimum 41.75 % H_2 at RSM- CCD optimized conditions of 703 ºC temperature, 1.45 g microalgal biomass loading, 22 ºC/min heating rate and 0.29 equivalent ratio (Raheem et al., 2015).

Analyzing TG-FTIR spectrum for gas evolutions with time and temperature variation, it is confirmed that pyrolysis temperature has significant effect upon syngas distribution (%). The thermodynamic assessment of coal and de-oiled microalgae pyrolysis showed that at lowest end of pyrolysis (200-300 °C), microalgae biomass with high H/C act as hydrogen donor to stabilize large radicals released from coal volatiles with negligible syngas production in agreement with reported studies (Gouws et al., 2021). The overall absorption intensity for volatiles is higher for ANN-MOGA optimized co-pyrolysis than RSM optimized (Fig. 6.11). Oppositely, CL ALG 1-1 sample (blending ratio: 50%) performed very poor emission (Fig. 6.11). Visualizing 3D infrared spectra at different optimization conditions, it is clear that above 350 ºC temperature, syngas emission is

progressively increased with pyrolysis temperature (Fig. 6.12). At initial stage of pyrolysis (Tp_1), methanation reactions outperformed with 38–42.23 % CH_4 production at different processing conditions as shown in Fig. 6.10. The H_2 selectivity is progressively increased at pyrolysis temperature of 400–600 °C. Hence, mid pyrolysis stage (Tp_2) is the main contributor for H_2 rich syngas emission than other characteristic temperatures (Tp_1 and Tp_3). Beyond 600–650 °C, CO_2 emission is more significant with sharply decreasing H_2 selectivity (Fig. 6.10). The maximum fraction of CO_2 is emitted at the last stage of pyrolysis (Tp_3) with very slight difference at RSM and ANN-MOGA optimized conditions showing 75.76 % and 74.07 % emission, respectively (Fig. 6.10).

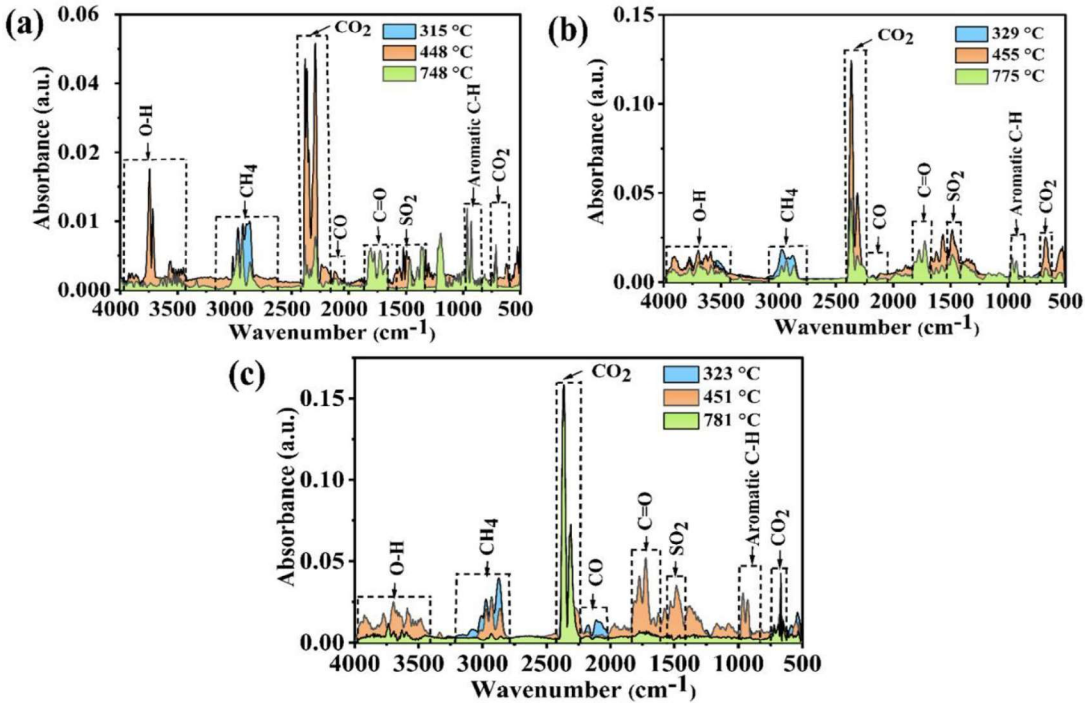

Fig. 6.11 TG-FTIR spectrum for gaseous product emission at different pyrolysis characteristic temperatures for (a) CL ALG 1-1 (blending ratio: 50%) (b) statistical optimized (RSM) (c) ANN-MOGA optimized condition.

Previous pyrolysis and gasification studies indicate that maximum emitted H_2 % in syngas has lied in the range of 9.5 to 42.88 % during pyrolysis of different biomass feedstocks such as microalgal species, i.e., *S. platensis* (Stucki et al., 2009), *C. vulgaris*

(Maliutina et al., 2017), *Scenedesmus* sp. (Beneroso et al., 2013) and lignocellulosic biomass; i.e., Sugarcane bagasse (Raheem et al., 2015) and Palm kernel shell (Maliutina et al., 2017).

In the direction of co-pyrolysis, Jun et al. (2017) investigated that 600 ºC pyrolysis temperature and 25 % blending of wheat straw with municipal solid waste promotes the cracking of macromolecular-hydrocarbons which yields H_2-rich syngas. In the co-pyrolysis of sub-bituminous coal and lignocellulosic biomass, an excessive CO_2 environment stimulates the thermal cracking of volatile organic compounds and yields enhanced syngas emission with significant H_2 production (Cho et al., 2016).

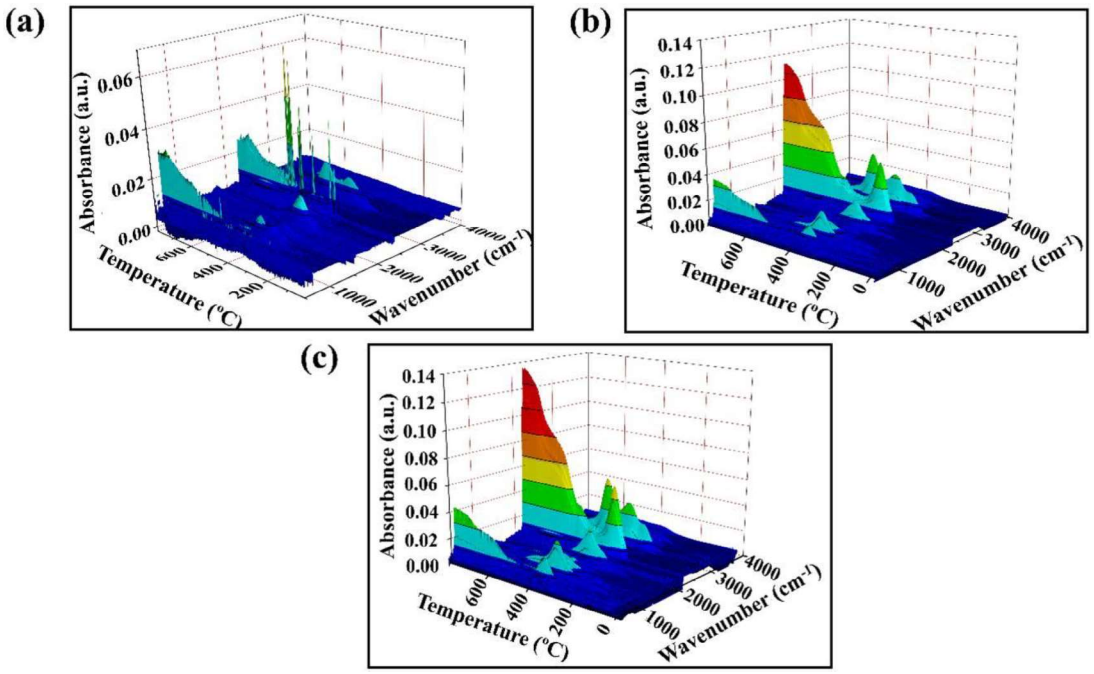

Fig. 6.12 3-D infrared spectra for multi-objective optimization to maximize hymethane carrying ratio at (a) CL ALG 1-1 (blending ratio: 50%) (b) statistical optimized (RSM) (c) ANN-MOGA optimized condition.

6.4 Conclusion

The co-pyrolysis of coal and de-oiled microalgae had been successfully modeled to enhance cumulative H_2 and CH_4 % in syngas using RSM and ANN-MOGA as optimization

tools. The findings indicated de-oiled microalgae with high volatile matter (43.01 %) and low ash content (18.0 %) as suitable candidates to blend with coal and contribute significantly to H_2-rich syngas emission. De-oiled microalgae blending impacts positively and heating rate impacts moderately for hydrogen and methane rich syngas emission. Both optimization tools RSM and ANN-MOGA, facilitate better interaction between process parameters and output generation. Utilizing low-cost feedstocks such as coal and de-oiled microalgae for H_2 and CH_4 synthesis is recommended for establishing potential carbon-neutral thermochemical conversion technology due to wide-ranging applications such as heat and power production and as a supplement of natural gas. Therefore, in-depth analysis of syngas emission at different pyrolysis stages and incorporation of advanced data-driven machine learning tools for optimization will lead towards scale-up and commercialization of co-pyrolysis for syngas production as an alternative to fossil fuel-derived gasification approaches.